Few-Body Syst (2023) 64:24
https://doi.org/10.1007/s00601-023-01808-x

Rimantas Lazauskas

Numerical Aspects of Resonant States in Quantum Mechanics

Received: 23 January 2023 / Accepted: 21 April 2023 / Published online: 4 May 2023

Abstract In this manuscript a short review on the most popular numerical techniques in Quantum mechanics used to determine properties of the resonant states is presented. Some common ambiguities arising when theoretical calculations are compared with the experimental data are also highlighted.

1 Introduction

Resonance phenomenon has attracted considerable attention in recent years. In nuclear physics this interest is nourished by the emergence of radioactive beam facilities allowing to test nuclei at the edge of stability. In cold atom physics magnetic trap experiments now allows to tune molecular systems into resonant regime. One should notice however that analysis of the experimental data is far from being straightforward, in particular, when resonant states are broad. Experimental data of resonant systems is often interpreted employing Breit-Wigner formulae, which for broad resonances is inappropriate. This troublesome situation is often encountered for so called shape resonances, where one or few particles are trapped in the shallow wells around local minima of the effective interaction surface. These particles easily escape from these shallow wells, therefore such resonances are short lived – their eigenergies (S-matrix pole position in complex energy plane) have sizeable imaginary parts. S-matrix poles of such states are relatively far from the physical (experimentally accessible) region, limited to real energy axis. Distance of the pole from the physical domain limits its impact on the physical observables, while separating of its contribution from background effects becomes a very delicate task. Unfortunately density of states in light nuclei is low and thus one has very few states, the vast majority of which are broad resonances. This nourishes an interest in these broad and highly non trivial structures among few-body physics community. This manuscript tries to address this question presenting a brief overview of the most popular numerical methods in quantum theory allowing to determine parameters of the resonant states as well as making their qualitative assessment.

Throughout this review for a sake of comparison I will consider two-particle scattering in P-wave, subject to a local potential built as a sum of two Yukawa functions:

$$V(\lambda, r) = \lambda \left[678.1 \exp(-2.55r) - 166.0 \exp(-0.68r)\right]/r. \tag{1}$$

In the last expression the radial distance (r) is measured in fm, whereas the potential energy is obtained in MeV. This potential is moderated by dimensionless parameter λ. If one fixes reduced mass of the system to $\frac{\hbar^2}{2\mu}$ =27.647 MeV.fm^2, the last potential qualitatively well simulates experimental P-wave phaseshifts of n-^{3}H scattering. By fixing $\lambda = 1$ obtained potential reproduce rather successfully $J^\pi = 2^-$ phaseshifts of the n-^{3}H system, whereas with $\lambda = 0.75$ one simulates $J^\pi = 0^-$ ones. By varying strength parameter λ, for a P-wave

Rimantas Lazauskas
Université de Strasbourg, CNRS, IPHC UMR 7178, 67000 Strasbourg, France
E-mail: Rimantas.Lazauskas@iphc.cnrs.fr

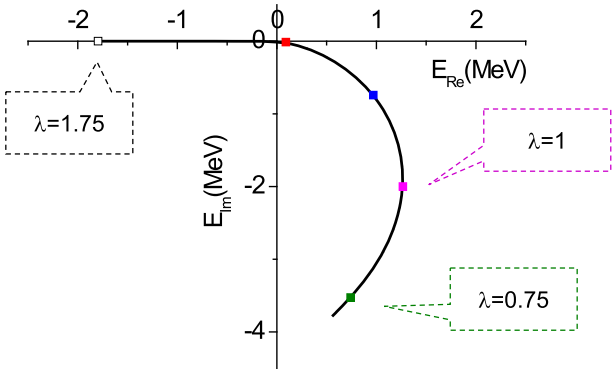

Fig. 1 Trajectory of the P-wave bound(resonant) state obtained by varying scale parameter λ for the potential defined in eq. (1)

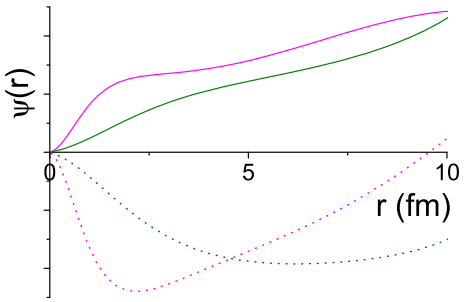

Fig. 2 Wave functions for the two broadest resonant states here considered, corresponding to λ =1.0 (pink curves) and λ =0.75 (olive) values respectively. Solid lines represent real and dotted imaginary parts of the wave functions

ground state one obtains a typical S-matrix pole trajectory (see Fig. 1) for a system described with non-zero orbital angular momentum. For $\lambda > \lambda_0$=1.52047 potential of (1) supports a P-wave bound state, whose energy increases smoothly with λ. Once decreasing while λ from its critical value bound state turns into resonant state, whose energy becomes complex and is situated in fourth quadrant. Resonant energy depicts a bended trajectory, which is result of absolute energy value $abs(E_{res})$ smoothly increasing while λ is reduced from its critical value λ_0 until S-matrix pole moves into third quadrant. At the same time real part of the energy $Re(E_{res})$ first is rapidly increasing, then stalls and finally starts rapidly decreasing.

In Fig. 2 real and imaginary parts of the resonance wave functions are presented for two cases of physical interest, $\lambda = 0.75$ and $\lambda = 1$. For these two cases centrifugal barrier, present in an effective potential, is not sufficient to trap systems wave function (for $\lambda = 1$ the height of repulsive barrier is only 1 MeV at its maximum) and thus concentration of the systems wave function near the origin is weak. This results corresponding S-matrix poles, see Fig. 1, to be situated far from the physical region (real energy axis) very broad resonant states, indicating that the formal lifetime of such a resonant state is extremely small. Separating contribution of such S-matrix poles on the physical observables is not straightforward. Typically, in the vicinity of the pole of S-matrix (resonance) scattering cross section reveals presence of a sharp variation, centered at scattering energy in center-of-mass frame $E_{cm} \approx \mathrm{Re}(E_{res})$. On contrary the centroids of elastic n-^{3}H P-wave cross section are shifted to considerably higher energies, while their widths do not match the corresponding $\mathrm{Im}(E_{res}) = \Gamma/2$ values. It is instructive, that while reducing λ value from $\lambda = 1$ to $\lambda = 0.75$ real part of E_{res} also gets smaller, while on contrary the centroid of elastic cross section moves to higher energy–see left panel of Fig. 3. In the right panel of the same figure dipole transition strengths

$$\frac{dB(E1)}{dE} = \frac{1}{E_k - E_0} \sum_{m\mu} |\langle \Psi_{klm} | r Y_{1\mu}(\Omega) | \Psi_0 \rangle|^2; \tag{2}$$

produced from a S-wave bound state at E=−4.606 MeV, described by wave function Ψ_0, generated by the same potential V(λ = 1,r) of Eq. (1) are displayed. Electric dipole operator ($rY_{1\mu}(\Omega)$) generates transition to a $l = 1^-$ continuum states (Ψ_{klm}) at energy $E_k = E + E_0$. The shapes of the dipole transitions reveal much more straightforward link with the position of the resonant state. Regardless the fact that $\mathrm{Re}(E_{res})$ values start

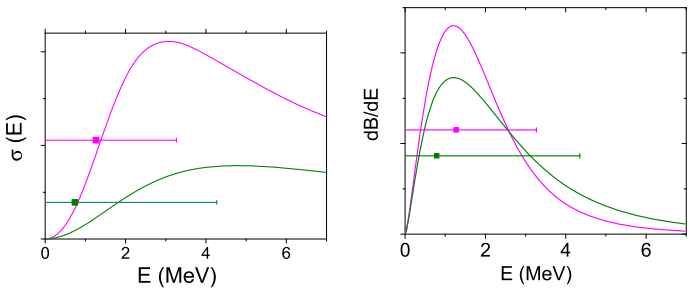

Fig. 3 Elastic cross section (left panel) and dipole response (right panel) functions in the resonance region for a potential of eq.(1) scaled by λ =1.0 (pink curves) and λ =0.75 (olive) values respectively, presented in arbitrary units. Corresponding resonance centroid and half-width are also provided for indication

decreasing with λ, the centroids of dipole strengths stalls with energy. However the widths of these centroids coincide much better with the calculated Γ values of the corresponding shape resonances than for elastic scattering cross sections. This behavior might be explained by the fact that for the dipole transitions initial state does not evolve with the energy and thus only indirectly affects the energy dependence. On contrary for the elastic scattering initial state strongly depends on the scattering energy, thus influencing directly the shape of the cross section.

In the following, based on the simple potential defined in eq.(1), five most popular methods employed to determine positions of the resonant states will be presented. Starting by the most rigorous and accurate direct method, continuing with very efficient Complex Scaling method and finishing by less accurate indirect approaches.

2 Direct Method

Resonant states are complex eigenvalues of the Hamiltonian, whose wave functions $\Psi(r) = \psi(r)/r$ contain only outgoing waves in the asymptote:

$$\psi(r \to \infty) = G(k_{res}r) + iF(k_{res}r) \propto e^{ik_{res}r}; \tag{3}$$

where $G(k_{res}r)$ and $F(k_{res}r)$ denote corresponding irregular and regular Coulomb functions. Since resonance wave momenta satisfy $Im(k_{res}) < 0$ relation, their wave functions diverge in far asymptote. The last fact complicates numerical determination of resonance position, making direct methods based on Hilbert space inappropriate. One is obliged either to use methods, which are able to handle properly diverging boundary conditions or try to determine resonance parameters indirectly.

The most straightforward way to determine resonance parameters is to solve corresponding Scrödinger equation by imposing appropriate outgoing wave behavior in the asymptote 3. For a set of problems limited to two-cluster open channels, this problem is easily handled by any method allowing to solve second order differential equation subject to non-vanishing boundary condition. One should solve:

$$(E - H_0 - V(r))\psi(r) = 0 \tag{4}$$

and search solutions satisfying boundary conditions for a regularized part of the systems wave function $u(r) = r\psi(r)$:

$$u(0) = 0 \tag{5}$$

$$u(r \to \infty) = [G(kr) + iF(kr)] + S^{-}(k)\,[G(kr) - iF(kr)]\,, \tag{6}$$

$$k = \sqrt{\frac{2\mu}{\hbar^2}E}. \tag{7}$$

In order to determine complex eigenenergy (E) of a resonant state, one should realize several solutions of Eq. (4) for different trial complex momentum-values (k) and scan the momentum surface for the points [1], where functional $S^{-}(k)$ (an inverse of a S-matrix) vanishes. Search procedure may be optimized by using gradient descent or Newtons methods. The only limitation of the direct method is related with the fact that one

should search momenta, which corresponds to the solution with incoming wave being absent in the asymptote. However, relative weight of the incoming to outgoing wave falls exponentially:

$$\left.\frac{G(kr) - iF(kr)}{G(kr) + iF(kr)}\right|_{r\to\infty} \propto e^{-2|\mathrm{Im}(k)|r}, \tag{8}$$

making numerical determination of the S-matrix poles with large $|\mathrm{Im}(k_{res})|$ become more and more delicate. On the other hand, large values of $|\mathrm{Im}(k_{res})|$ reflect that these S-matrix pole are situated far from the physical domain (real momentum axis) and thus does not play important role in shaping physical observables.

S-wave solutions present a particular case. S-wave poles stay on the imaginary momentum axis: by reducing potential strength parameter they are moving form its positive part (bound state solution) to negative one (virtual state). Regularized wevefunction of a bound/virtual state behaves in the asymptote, as:

$$u(r \to \infty) \propto \exp(ikr). \tag{9}$$

This particular problem might be solved by factorizing systems wave function:

$$u(r) = f(r)\exp(ikr), \tag{10}$$

and inserting this expression into Schrödinger equation (4), one gets:

$$\left[-\frac{d^2}{dr^2} + \frac{2\mu}{\hbar^2}V(r)\right] f(r) = k\left[2i\frac{d}{dr}\right] f(r) \tag{11}$$

satisfying boundary conditions:

$$f(0) = 0, \tag{12}$$

$$f'(r \to \infty) = 0. \tag{13}$$

One may solve directly the generalized eigenvalue problem of eq.(11) and determine the values of eigen-momenta k. There is no need anymore to scan the complex energy plane for the solutions satisfying proper boundary condition of eq.(6), which is imposed via Eq. (13). Numerical eigenenergies of the last equation will appear as complex conjugate pairs with some real-negative eigenvalues, corresponding to virtual/bound states.

One may also use the last technique in order to find rough estimate of the position of the resonant state for non-zero angular momentum $l > 0$. For this purpose we introduce an effective potential

$$V_{eff}(r) = \left[V(r) + \frac{\hbar^2}{2\mu}l(l+1)/r^2\right] H_{cut}(R_{\max} - r). \tag{14}$$

This effective potential coincides with a full potential in the large part of the configuration space but then is forced to vanish beyond some large radius $R_{\max}$ by means of function $H_{cut}(R_{\max} - r)$. The cut-off function $H_{cut}(R_{\max} - r)$ numerically should simulate Heaviside Delta function. Like for a standard S-wave potential, the outgoing wave solution then satisfies:

$$f'(r > R_{\max}) = 0 \tag{15}$$

The results employing the last technique are presented in Table 1. One may notice, that once cut-off radius is chosen sufficiently large the method works well both in estimating positions of the bound states as well as positions of narrow resonant states. Presence of non physical cut-off function, which abruptly cuts centrifugal barrier, results however calculated eigenvalues to oscillate with the cut-off range. Amplitude of these oscillations increases as a resonant state becomes broader, finally resulting in methods failure. In our studied example these oscillation makes identification of the broadest resonance position, provided by $\lambda = 0.75$, completely impossible.

Table 1 Estimation of the energy eigenvalues for a P-wave, when suppressing long range part of the centrifugal term and imposing S-wave boundary condition

$\lambda \setminus R_{max}$ (fm)	20	30	40	exact
1.75	− 1.8208	− 1.7929	− 1.7913	− 1.7914
1.5	$(5.73–2.82i)\cdot10^{-2}$	$(9.50–2.01i)\cdot10^{-2}$	$(9.62–1.51i)\cdot10^{-2}$	$(9.33–1.52i)\cdot10^{-2}$
1.25	$0.92–0.71i$	$1.02–0.71i$	$1.12–0.82i$	$0.9712–0.7446i$
1.0	$1.55–1.91i$	$1.16–1.78i$	$0.96–1.57i$	$1.267–2.002i$
0.75				$0.7429-3.530i$

Calculated eigenvalues are presented as a function of the interaction strength λ and the cut-off range parameter R_{max} (fm) in Eq. (14) In the last column exact numerical values are presented for comparison

3 The Complex Scaling Method

Unfortunately, a domain of application for a direct method is very limited. Composite particle systems dispose several open channels and thus their wave functions may reveal very complex behavior in the asymptote. Resonant state in such systems thus also involve multiple decay channels, which may break into more than two clusters. Regardless these complications, complex scaling method allows to solve problem of multiparticle resonant states very efficiently and requires only moderate effort to be implemented. In view of rich available literature on the subject this method will be described here very briefly, for more complete review one may refer to [2–4].

A full equivalent of the complex scaling (CS) method has been developed already during the World War II by D.R. Hartree et al. [5,6] in relation with the study of the radio wave propagation in the atmosphere. D.R. Hartree et al. were interested in complex eigenvalues of the second order differential equations describing radio wave propagation. Technically this problem is equivalent to one of finding S-matrix pole positions, in relation with the resonant states of quantum two-particle collision process. In the late sixties J. Nuttal and H. L. Cohen [7] proposed a very similar method to treat the general scattering problems, dominated by the short range potentials. A few years later E. Baslev and J. M. Combes [9,10], analyzing eigenvalue structure of the CS Hamiltonian, provided mathematical foundation for the CS method. In this way the original method of D.R. Hartree has been recovered in order to determine resonance eigenvalues in atomic physics [2,3].

The vast majority of the computational methods in quantum mechanics has been developed for the Hermitian operators. However, the physical Hamiltonians are Hermitian only when they operate on bounded (square integrable) functions. Wave functions describing resonant states or particle collisions does not meet the last criteria. Nevertheless, an extension of the variational principle and of the other well-known theorems in quantum mechanics to the non-Hermitian operators can be made by carrying out similarity transformations $\widehat{S}$, which converts outgoing scattered waves, ϕ^{out}, into the square integrable functions. That is,

$$E\left(\widehat{S}\psi\right) - \left(\widehat{S}\widehat{H}\widehat{S}^{-1}\right)\left(\widehat{S}\psi\right) = \widehat{S}I, \tag{16}$$

such that

$$\widehat{S}\psi^{out}(r \to \infty) \to 0; \tag{17}$$

function $\widehat{S}\psi^{out}(r)$ belongs to the Hilbert space although $\psi^{out}(r)$ does not. The complex-scaling operator to be defined below is only one example of a vast set of similarity transformations for which the last relation is satisfied. However simplicity of the complex-scaling operator and its conformity with the existing numerical methods makes it unmatched in the practical applications.

The complex-scaling (CS) operator is defined as

$$\widehat{S} = \exp(i\theta r\frac{\partial}{\partial r}), \tag{18}$$

such that

$$\widehat{S}f(r) = f(re^{i\theta}). \tag{19}$$

Of particular interest is an action of this operator on the outgoing scattered waves

$$\widehat{S}\phi^{out}(r\to\infty)\propto\exp(ikre^{i\theta})=\exp(i\,|k|\,re^{i\theta}), \tag{20}$$

as before, here k denotes the scattering momentum.

CS transformation of the Hamiltonian is also rather trivial. For a sake of clarity, and without loss of generality, let us consider the one-dimensional radial Hamiltonian. When the potential is dilution analytic, the complex-scaled Hamiltonian is simply:

$$H_l^\theta=\widehat{S}\widehat{H}\widehat{S}^{-1} \tag{21}$$

$$=-\frac{\hbar^2}{2\mu}\frac{d^2}{e^{2i\theta}dr^2}+\frac{\hbar^2}{2\mu}\frac{l(l+1)}{e^{2i\theta}r^2}+V(re^{i\theta}). \tag{22}$$

From the last expression it follows that the CS transformation simply scales kinetic energy operator by a factor $e^{-2i\theta}$, i.e.:

$$T_{ij}^\theta=\frac{1}{e^{2i\theta}}T_{ij} \tag{23}$$

Calculation of the potential energy matrix is more complicated, but still rather trivial. For the local potential one has:

$$V_{ij}^\theta=\left\langle f_i\left|\widehat{S}\widehat{V}\widehat{S}^{-1}\right|f_j\right\rangle=\int_0^\infty f_i(r)V(re^{i\theta})f_j(r)dr \tag{24}$$

If the potential is non-local $V(r,r\prime)$:

$$V_{ij}^\theta=\int_0^\infty e^{i\theta}f_i(r)V(re^{i\theta},r'e^{i\theta})f_j(r')drdr' \tag{25}$$

One may refer to the [4,11] for a more detailed discussion on the CS transformation of the potential energy.

Two-particle resonant state wave functions are defined by the outgoing wave solutions Eq. (3). It is of particular interest to express an action of the complex scaling operator on a wave function of a resonant state:

$$\widehat{S}\psi_n^{res}(r\to\infty)\propto\exp(ik_n^{res}re^{i\theta})=\exp(i\left|k_n^{res}\right|re^{i(\theta-\vartheta^{res})}) \tag{26}$$

$$=\exp(i\left|k_n^{res}\right|r\cos\left(\theta-\vartheta^{res}\right))\exp(-\left|k_n^{res}\right|r\sin\left(\theta-\vartheta^{res}\right)) \tag{27}$$

It follows, that the complex-scaled resonance wave functions become exponentially bound if a condition

$$\mathrm{mod}(\theta-\vartheta^{res},2\pi)<\pi \tag{28}$$

is satisfied.

It is of interest to see how a CS transforation affects the spectra of the Hamiltonian. According to the Aguilar, Balslev and Combes (ABC) theorem [9,10], see Fig. 4:

1. The bound state poles remain unchanged under the transformation.
2. The cuts are now rotated downward making an angle of 2θ with a real axis.
3. The resonant poles are "exposed" by the cuts once the angle θ is larger than $-\frac{1}{2}Arg(E_{res})$, where E_{res} is the complex eigenenergy value of a resonant state.

It is easy to prove this theorem for short-range potentials. In such a case, the scattering states have asymptotic behavior given by:

$$\psi^{scatt}(r\to\infty)=A(k)e^{-ikr}+B(k)e^{ikr} \tag{29}$$

where as usual, center-of-mass kinetic energy (E) can be expressed in terms of the momentum (k), via:

$$E=\frac{\hbar^2}{2\mu}k^2. \tag{30}$$

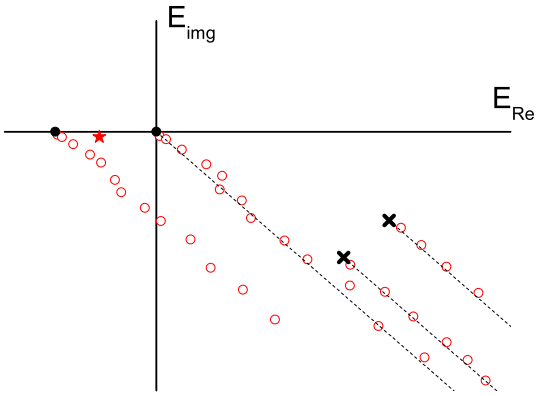

Fig. 4 Typical spectrum of the complex scaled Hamiltonian. Solid black points indicate positions of the thresholds and by crosses position of resonant states in the subsystems. From these points extends lines, rotated clockwise by angle 2θ relative to real energy axis. Complex-Hamiltonian eigenvalues corresponding to discredited continuum are scattered along these lines. Genuine resonant state is marked by a star symbol – it is separated from the rotated continuum lines

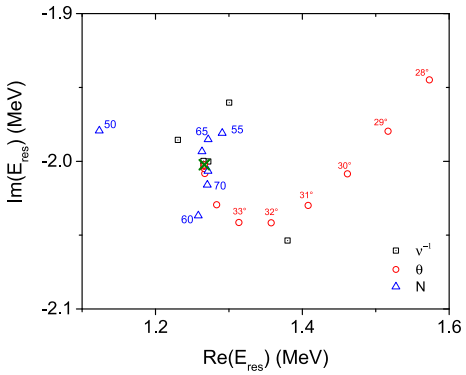

Fig. 5 Calculation of resonant state position using CSM for a potential of Eq. (1) scaled by $\lambda = 1$. Several calculation rounds are performed: varying number of Laguerre basis functions (N), varying range of the Laguerre exponent (ν^{-1}) and by changing CS angle (θ). Exact position of a resonant state is indicated by a cross symbol

The energy can take any real positive value, provided that the threshold energy is taken as zero. The CS operator transforms scattering state wave function as

$$\widehat{S}\psi^{scatt}(r \to \infty) = A(k)e^{-ikre^{i\theta}} + B(k)e^{ikre^{i\theta}}. \tag{31}$$

The transformed wave functions diverge if $\theta < \pi$, due to the real part of the exponential factor $e^{-ikre^{i\theta}}$ being positive. The only non exponentially divergent functions are obtained when k gets complex values,

$$k = |k|\, e^{-i\theta} \tag{32}$$

and therefore, if the threshold is taken as the zero reference energy,

$$E = |E|\, e^{-i2\theta}. \tag{33}$$

According to the ABC theorem [9,10] in order to find the resonant states one should simply solve a eigenvalue problem for a complex Hamiltonian:

$$H_l^\theta \widetilde{\psi}_n^\theta(r) = E_n^\theta \widetilde{\psi}_n^\theta(r), \tag{34}$$

keeping in mind that the resonant eigenvalues are "exposed" by the cuts of the rotated continuum states, when $\theta > -\frac{1}{2}Arg(E_R)$.

The complex analog to the variational principle provides a formal justification to the use of the computational techniques that originally were developed for the bound states. The Rayleigh quotient

$$E_n^\theta = \frac{(\psi \left| H_l^\theta \right| \psi)}{(\psi \,|\psi)} \tag{35}$$

provides a stationary approximation to the true complex eigenvalue E_n^θ when ϕ is a c-normalizable eigenfunction of H_l^θ, which is close to exact solution $\widetilde{\phi}_n^\theta(r)$. This means that the calculated eigenvalues, corresponding to some resonant state, will stabilize around the exact solution without providing any bound (upper, lower) for the eigenenergy.

In practice convergence of the calculated resonance eigenvalues might be improved by either increasing a size of the eigenfunction basis (or density of the wave-function discretization points), or by increasing the complex scaling angle beyond its critical value $\theta = -\frac{1}{2}Arg(E_R)$. The physical resonance eigenvalues frequently appear close to the thresholds and therefore the values of $\left|k_n^{res}\right|$ in eq.(27) are usually small, resulting slow decaying exponent for the CS resonant wave functions. At the same time due to the presence of the exponent $\exp(i\left|k_n^{res}\right| r\cos(\theta - \vartheta^{res}))$ these asymptotes might be strongly oscillating. This demonstrates that much of the care should be taken in describing the far-extending parts of the resonant wave functions.

In Fig. 5 calculation of the P-wave resonant eigenvalue, corresponding to potential of Eq. (1) defined by λ=1.0, using CS method is presented. Three rounds of calculation are realized by varying number of Laguerre basis functions (N), varying range of the Laguerre exponent (ν^{-1}) and by changing CS angle (θ). As pointed out calculated eigenvalues concentrate near the exact one, indicated by a cross and found using direct method. By increasing either size of the basis or CS angle (θ) calculated eigenvalues approach exact one, however there is no defined direction for the convergence. Argument of the resonant eigenvalue $\vartheta^{res} \approx 28.8^\circ$ and thus CS angle θ well beyond 30° is required to get converged result.

These developments might be easily extended in order to handle a problem of few-particle resonant states, one must simply keep in mind that a multiparticle resonance wave function might involve more than decay channels, related with a presence of more than one scattering threshold. Nevertheless very similar condition, as one formulated for a 2-body case in Eq. (28), should be validated. This condition however should be satisfied relative to each open decay channel. Furthermore one should be aware of the possible appearance of the discretized continuum pseudostates, associated with a presence of the resonant states in the subsystems (see Fig. 4). In the complex energy plane these pseudostates are scattered along the lines starting from the resonant energy of the subsystem and rotated by an 2θ angle relative to the real energy axis.

There are many different modifications of the complex scaling method, which might be very useful to handle specific problems. As example, short-ranged potentials often have repulsive cores, which poses severe difficulties for CS transformation. For a two-body problems this obstacle is easily overcome by modifying transformation (18) in such a way that it does not affect short range region – giving rise to so called exterior complex scaling technique [12]. Nevertheless these modifications are much less universal than conventional CSM and might pose serious difficulties when extending it beyond A=2 case. For those interested in this subject may address to more specific review [4,11].

4 Extrapolation Techniques

If the tools to calculate S-matrix on the physical axis are available, one may employ extrapolation technique to determine S-matrix poles. S-matrix is unitary on real axis but should diverge at its poles, therefore close to its poles its behavior may be described by [13]:

$$S_L(k) = e^{2i\delta_L(k)} = \frac{k - k^*_{res}}{k - k_{res}}, \tag{36}$$

where $\delta_L(k)$ is the scattering phaseshift at orbital angular momentum L, determined for scattering momentum k. On the other hand, at low energies scattering phaseshifts behave according to effective range expansion (ERE):

$$k^{2L+1}\cot(\delta_L(k)) = -\frac{1}{a_L} + \frac{1}{2}r_L k^2 + c_i k_{res}^{2i+2} + .., \tag{37}$$

Table 2 Resonance position for $\lambda = 1.0$ extracted by fitting ERE (37) by increasing number of expansion coefficients n=i+2. In the second column residual sum of squares (RSS) of ERE is given. Extracted resonance eigenvalues are compared with an exact one

i	RSS	E_{res} (MeV)
0	$1.1 \cdot 10^{-8}$	1.4864-1.9780i
1	$1.2 \cdot 10^{-11}$	1.2612-1.9981i
2	$6.2 \cdot 10^{-13}$	1.2661-2.0031i
exact		1.2666-2.0023i

combining the two last expressions, one gets non linear equation to determine potential positions of the S-matrix poles k_{res} :

$$ik_{res}^{2L+1} = -\frac{1}{a_L} + \frac{1}{2} r_L k_{res}^2 + c_i k_{res}^{2i+2} \ldots \tag{38}$$

The real S-matrix poles, corresponding to resonance positions, will be stable solutions of the last equation, which converge by increasing order of ERE. As a consequence of the finite truncation of the ERE, other roots of the non-linear equation (38) will vary strongly with the order of ERE. This observation leads us to a simple procedure in order to determine positions of the resonant state:

1. Solve scattering problem and determine S-matrix values for several scattering momenta k
2. Determine ERE parameters: a_L, r_L, c_i, with $i \geq 1$.
3. Solve non-linear equation (38) and determine k_{res}, the stable solutions relative to order of ERE expansion.

As alternative to ERE, one may parameterize scattering amplitude employing Padé expansion, as:

$$k^{2L+1} cot(\delta_L(k)) = -\frac{P_N(k_{res}^2)}{Q_M(k_{res}^2)}; \tag{39}$$

where $P_N(x)$ and $Q_M(x)$ are real coefficient polynomials of x of order N and M respectively. One should additionally impose $Q_M(0) = 1$, to avoid linear dependence of two polynomials. ERE parametrization works perfectly if scattering process is limited to elastic one, whereas Padé expansion is preferential for more complex cases, where standard ERE is not appropriate. Padé expansion technique has been used very successfully in determining parameters of three and four body resonant states [14,15].

As an example in Table 2. In Fig. 6 fit of scattering phaseshifts is demonstrated by limiting ERE to two terms only: scattering volume (a_L) and effective range (r_L), i.e. i=0. This is sufficient to obtain very accurate description of the phaseshifts, nevertheless calculated resonance position is still by 15% off the exact value. Clearly for more pronounced resonant states, residing closer to the real energy axis, less effort is needed to determine resonance position. In conclusion, accurate knowledge of the phaseshifts empowers one to extract even positions of broad resonant states.

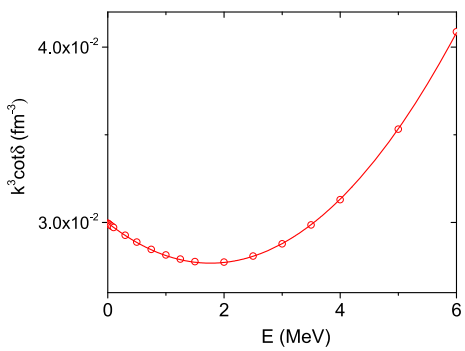

Fig. 6 Fitting effective range expansion (37) using second order polynomial, i.e. i=0

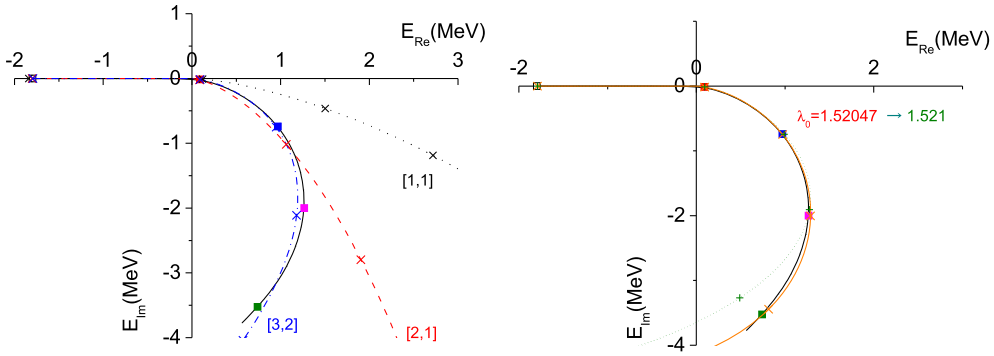

Fig. 7 Application of the ACCC method to extract resonance positions from the calculated binding energies obtained for potential of Eq. (1)

5 ACCC Method

Many numerical techniques in physics are limited to Hilbert space and thus are not appropriate to solve the boundary condition problems, required to determine scattering observables. In [16–18] V.I. Kukulin et al. proposed a method of analytic continuation in the coupling constant (ACCC) in order to derive trajectory of a resonant state as a function of the potential coupling constant. This method requires only to collect a data from the bound state calculation. It is based on the intuitive argument that resonance may be treated as an eigenstate of a system which arises from a bound state, when the intensity of the attractive part of the interaction decreases. S-matrix pole of a resonant-state is defined as the analytic continuation of a bound-state pole in the coupling constant of the attractive part of the total Hamiltonian. I.e. one assumes that systems Hamiltonian can be written as $H(\lambda) = H_0 + \lambda H_{att}$, where H_{att} is an attractive part of unperturbed Hamiltonian $H(\lambda = 1.0)$. If for some λ Hamiltonian possess a bound state then, by gradually decreasing λ, this bound state approaches threshold $E(\lambda_0) = 0$ and becomes a resonant or virtual one.

For a physical Hamiltonian binding energy should be analytic in λ. Moreover, it can be shown [18], that for a two-body system the square root of the binding energy near the threshold E(λ_0)=0 behaves as:

$$k_\ell = \sqrt{-E} \sim x \equiv \begin{cases} \lambda - \lambda_0 & \text{for} \quad \ell = 0 \\ \sqrt{\lambda - \lambda_0} & \text{for} \quad \ell \neq 0 \end{cases} \tag{40}$$

Therefore one can consider k_ℓ as a analytical function of x and analytically continue this function from bound state region ($\lambda > \lambda_0$) into resonance region ($\lambda < \lambda_0$). Motivated by the functional (40) of the k_ℓ near the threshold, one can use Padé approximation [19]:

$$k_l(x) = k^{[N,M]}(x) = \frac{a_1 \cdot x + a_2 \cdot x^2 + \ldots a_N \cdot x^N}{1 + b_1 \cdot x + b_2 \cdot x^2 + \ldots b_M \cdot x^{M-1}} \tag{41}$$

One may easily generalize this method for a n-particle system. In this case, k_ℓ denotes a relative momenta to the nearest particle threshold $k = \sqrt{-(E_n - E_{i<n})}$. However, in contrary to n=2 case, systems angular momentum not anymore solely determines if bound state turns into virtual or resonant state, when $\lambda < \lambda_0$. If at critical point resonant state breaks in two clusters with relative momentum $\ell = 0$ – then virtual state is formed, otherwise bound state turns into resonant one. Alternatively, according to Eq. (40), properties of this transition can be determined by studying nearthreshold behavior of binding energies $\sqrt{-(E_n - E_{i<n})}$. If $(E_n - E_{i<n})$ is linear in $(\lambda - \lambda_0)$ at the origin – bound state turns into a resonance; virtual state appears if $(E_n - E_{i<n})$ is quadratic in $(\lambda - \lambda_0)$.

In Fig. 7 trajectories obtained for potential of eq.(1) are depicted. Resonant state trajectories have been determined by fitting N+M Padé expansion coefficients of eq.(41) for a data of 19 binding energies collected in the interval -20 MeV$< E(\lambda) <$0. The critical strength parameter λ_0=1.52047 has been determined very accurately solving scattering problem at zero energy and searching for divergence of the scattering length. One may see that exact resonance trajectory, obtained using direct method, might be accurately reproduced but it requires determination of high order Padé approximants. The last feature imposes stringent constrain on the accuracy of the collected binding energy data: the average deviation of the fitted binding energies from the Padé parametrization, depicted in the Fig. 7, of order [M,N]=[1,1], [2,1] and [3,2] are respectively 0.13 MeV,

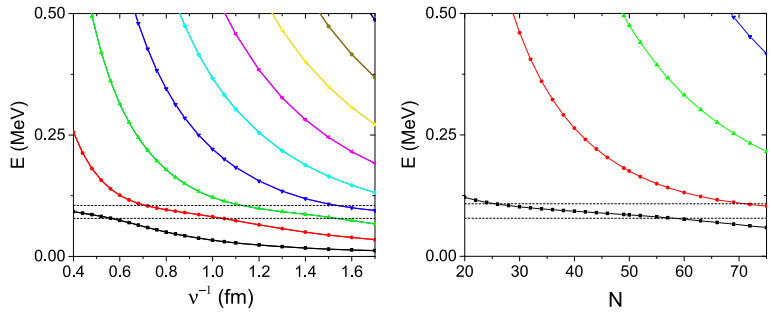

Fig. 8 Demonstration of the stabilization method. Calculated eigenvalues of the Hamiltonian are depicted as a function of range (ν^{-1}) parameter of the employed Laguerre-basis (left panel) and of the number of basis functions used (right panel). A case of a narrow resonance $E_{res} = (9.33 - i\,1.52)\cdot 10^{-2}$ MeV is studied, obtained for a potential (1), defined with λ_0=1.5. Dashed-horizontal lines indicate resonance range E=Re(E_{res})$\pm\Gamma/2$

0.01 MeV and $6\cdot 10^{-5}$ MeV only. Resonance trajectory for $\lambda \lesssim \lambda_0$ (vicinity of real energy axis) is reproduced quite straightforwardly, however important effort is required to reproduce a proper bending of the resonance trajectory and thus positions of the broad resonant states. Furthermore, methods accuracy heavily depends on how well critical strength parameter λ_0 is determined. In the right panel of Fig. 7 input value for this parameter is changed in a fifth digit to 1.521. The comparison is realized for Padé approximants of order [M,N]=[5,4]. The small shift in employed strength parameter λ_0 results in a small deterioration of the fitted binding energies, average deviation dropped from 10^{-7} MeV to $2.7\cdot 10^{-7}$ MeV. This results however in significant deterioration of the reproduced resonance trajectory in its distant part.

One should remark that determination of the λ_0 value presents also the most difficult task when using conventional bound state techniques. One has increasing difficulty in determining binding energies of the system close to its critical point, due to large extensions of the wave function.

As demonstrated in [20–23], one may also apply ACCC beyond 2-body problem. However, naive scaling of 2-body interaction is not appropriate in this case; as this procedure does not preserve threshold positions, associated with a possible existence of bound states in the subsystems. New thresholds may arise, associated with formation of bound states in the subsystems, while threshold dependence on strength parameter invalidates approximation in (41). To avoid these complications in [21–23] one chose to add attractive many-body force, which does not act in the subsystems, and express parametrization (41) as a function of a strength parameter of this auxiliary force. When applying the last technique however, very careful choice of auxiliary force is needed, trying to maximize its overlap with the original Hamiltonian and wave function of a resonant state. Otherwise situation may arise, where the auxiliary force creates a set of bound states by itself and newly produced bound state does not evolve into the resonant state of interest, when removing this force.

6 Stabilization Method

It is well known, that if a system has a narrow resonant state at energy E_{res} with a width $\Gamma << E_{res}$, then scattering wave function in the energy range ($E_{res} - \Gamma/2$,$E_{res} + \Gamma/2$) will be strongly localized at the origin, retained by the potential barrier and only small fraction of the flux penetrates this barrier outside. In this way the resonance wave function strongly resemble bound state one and its internal part may be successfully approximated by the square integrable basis functions. Furthermore, variational principle should hold up to a certain level and calculated eigenvalues of the Hamiltonian should demonstrate some stability relative to variational parameter in the vicinity of a resonance energy as suggested in [24,25].

The method is based in the observation that when varying variational parameter ν or number of the square integrable basis states, the eigenvalue corresponding to the real part of a resonant state (E_{res}) has an avoided crossing with the real eigenvalues corresponding to the continuum (E_c). The analysis of this level repulsion near the crossing point, defined by the intersection of the asymptotes to both curves, provides an estimation of the resonance parameters (E_{res}, Γ).

In Fig. 8, the level crossing between a resonant state (E_r) and a continuous state (E_c) moving down, is produced at $\alpha = \alpha_c$ and defines the resonant energy E_R (dashed horizontal line). This feature is a signature of

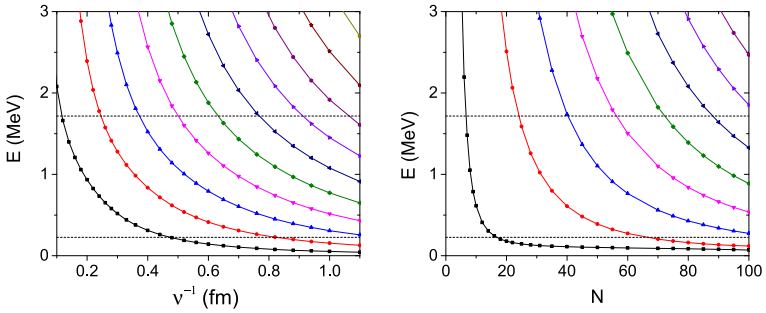

Fig. 9 The same as in Fig. 8 but for a broader resonant state $E_{res} = 0.9712 - 0.7446i$ MeV, defined with λ_0=1.25

a resonance state of the Hamiltonian with real energy E_R and a width given by [25]

$$\Gamma = 2\Delta E \, \frac{\sqrt{|\, S_r \,||\, S_c \,|}}{|S_r - S_c|} \tag{42}$$

where ΔE (in red) is the energy difference between the two curves at the crossing, and S_r and S_c are respectively the slopes of the resonant and continuous levels asymptotes at the crossing.

The stabilization method, is closely connected with the ACCC method, but lacks of a sound mathematical ground, providing only rough estimation of the resonance width. This method has been recently applied, in conjunction with the Gaussian Expansion Method, to determine the resonance positions of a doubly heavy tetraquark system [26] as well as studying potential existence of a narrow resonant state in ^{7}H nucleus [27]. Nevertheless as demonstrated in Fig. 9 stabilization method might be difficult to apply in searching broad resonant states.

Acknowledgements In preparing this manuscript I have benefited from the grant of French CNRS/IN2P3 for a theory project "Neutron-rich light unstable nuclei". I was also granted access to the HPC resources of TGCC/IDRIS under the allocation A0110506006 made by GENCI (Grand Equipement National de Calcul Intensif). Part of this manuscript has been prepared during the program Living Near Unitarity at the Kavli Institute for Theoretical Physics (KITP), University of Santa Barbara (California) is supported in part by the National Science Foundation under Grant No. NSF PHY-1748958.

References

1. M.T. Pena, A.C. Fonseca, Use of splines to calculate resonance poles and Gamow states. Phys. Rev. C **36**(5), 1737 (1987)
2. Y.K. Ho, The method of complex coordinate rotation and its applications to atomic collision processes. Phys. Rep. **99**(1), 1 (1983)
3. N. Moiseyev, Quantum theory of resonances: calculating energies, widths and cross-sections by complex scaling. Phys. Rep. **302**(5–6), 212–293 (1998)
4. R. Lazauskas, arXiv:1904.04675 (2019)
5. R. Hartree, J.G.L. Michel, N.P., Meteorological factors in radiowave propagation, Report of a Conference held on 8th April 1946 at The Royal Institution, London by The Physical Society and The Royal Meteorological Society (The Physical Society, London), pp. 127–168 (1946)
6. J.N.L. Connor, Scattering amplitude without an explicit enforcement of boundary conditions. J. Chem. Phys. **78**, 6161 (1983)
7. J. Nuttal, H.L. Cohen, Method of complex coordinates for three-body calculations above the breakup threshold. Phys. Rev. **188**, 1542–1544 (1969)
8. F.A. McDonald, J. Nuttall, Neutron-deuteron elastic scattering above the breakup threshold. Phys. Rev. C **6**, 121–125 (1972)
9. J. Aguilar, J.M. Combes, A class of analytic perturbations for one-body Schrödinger Hamiltonians. Commun. Math. Phys. **22**, 269 (1971)
10. E. Balslev, J.M. Combes, Spectral properties of many-body Schrödinger operators with dilatation-analytic interactions. Commun. Math. Phys. **22**, 280 (1971)
11. T.N. Rescigno, M. Baertschy, W.A. Isaacs, C.W. McCurdy, Collisional breakup in a quantum system of three charged particles. Science **286**(5449), 2474–2479 (1999)
12. B. Simon, The definition of molecular resonance curves by the method of exterior complex scaling. Phys. Lett. A **71**(2), 211–214 (1979)
13. J. R. Taylor, Scattering Theory: The Quantum Theory of Nonrelativistic Collisions, Courier Corporation (2006)
14. A. Deltuva, Three-neutron resonance study using transition operators. Phys. Rev. C **97**(3), 034001 (2018)
15. A. Deltuva, Tetraneutron: Rigorous continuum calculation. Phys. Lett. B **782**, 238–241 (2018)
16. V. Kukulin, V. Krasnopolsky, Description of few body systems via analytical continuation in coupling constant. J. Phys. A **10**, L33–L37 (1977)

17. V. Krasnopolsky, V. Kukulin, Theory of resonance states based on analytical continuation in the coupling constant. Phys. Lett. A **69**(4), 251–254 (1978)
18. V.I. Kukulin, V.M. Krasnopolsky, J. Horácek, *Theory of Resonances: Principles and Applications* (Reidel Texts in the Mathematical Sciences, Springer, Netherlands, 1989)
19. Jr, G. A. Baker, The theory and application of the Padé approximant method,Los Alamos Scientific Lab., Univ. of California, N. Mex. (1964)
20. A. Hemmdan, W. Gløckle, H. Kamada, Indications for the nonexistence of three-neutron resonances near the physical region. Phys. Rev. C **66**, 054001 (2002)
21. R. Lazauskas, J. Carbonell, Three-neutron resonance trajectories for realistic interaction models. Phys. Rev. C **71**, 044004 (2005)
22. R. Lazauskas, J. Carbonell, Is a physically observable tetraneutron resonance compatible with realistic nuclear interactions? Phys. Rev. C **72**, 034003 (2005)
23. R. Lazauskas, E. Hiyama, J. Carbonell, Ab initio calculations of 5H resonant states. Phys. Lett. B **791**, 335 (2019)
24. H.S. Taylor, Models, interpretations, and calculations concerning resonant electron scattering process in atoms and molecules. Adv. Chern. Phys. **18**, 91 (1970)
25. J. Simons, Resonance state lifetimes from stabilization graphs. J. Chem. Phys. **75**(5), 2465–2467 (1981)
26. Q. Meng, M. Harada, E. Hiyama, A. Hosaka, M. Oka, Doubly heavy tetraquark resonant states. Phys. Lett. B **824**, 136800 (2022)
27. E. Hiyama, R. Lazauskas, J. Carbonell, 7H ground state as a 3H+ 4n resonance. Phys. Lett. B **833**, 137367 (2022)